TWO-PHASE FLOW IN CHANNELS WITH NON-CIRCULAR CROSS-SECTION OF PNEUMATIC TRANSPORT OF POWDER MATERIAL

by

Saša M. MILANOVIĆ**, Miloš M. JOVANOVIĆ, Živan T. SPASIĆ, and Boban D. NIKOLIĆ

Faculty of Mechanical Engineering, University of Nis, Nis, Serbia

Original scientific paper
https://doi.org/10.2298/TSCI18S5407M

The paper presents a numerical simulation of two-phase turbulent flow in straight horizontal channels of pneumatic transport with non-circular cross-section. For the granular flow simulation, we have chosen the flow of solid particles of quartz, flour, and ash in the flow of air, which is transporting fluid. During the modeling of the flow, the transported solid particles are reduced to spherical shapes. A correction of the stress model of turbulence is performed by taking into account the influences of the induction of secondary flows of the second order in the gas phase. The full Reynolds stress model was used for modeling the turbulence, and the complete model is used for the turbulent stresses and turbulent temperature fluxes. All numerical experiments were conducted for the same initial flow conditions and a single uniform grid was adopted for all numerical experiments. The flow is observed in a straight channel of a square cross-section and dimensions of sides of 200 mm and the length of 80 D_h. During the simulation, the fineness of the numerical grid was also tested, and the paper shows results of the numerical grid of the highest resolution beyond which the fineness does not influence the obtained results. The paper offers graphics of velocities of the solid particles transported by the transporting fluid (air) along the channel.

Key words: *computer simulation, pneumatic transport, solid particles, channel, two-phase flow*

Introduction

Pneumatic transport means the transport of loose, granular or powder material mostly using the flow of air or some other gas. The transport of material is based on the fact that the air-flow acts upon solid particles with aerodynamic forces, which become sufficiently strong at certain air velocities so as to lift and move the transported material particles. The motion of particles of material in the pneumatic transport is chaotic and with collisions, yet with a basic component of velocity along the channel which is lower than the velocity of the transporting air.

Two-phase flows of the air-solids type in channels with a non-circular cross-section are frequent in engineering. The most common examples of this type of flow appear in systems of pneumatic transport of granular and powder material, in air conditioning and ventilation systems, process and energy systems, *etc.* In general sense, two-phase flows are charac-

* Corresponding author, e-mail: msasa@masfak.ni.ac.rs

terized by a special complex of flow phenomena that result from interactions between the gas and the solid phase, chemical reactions between the phases, the elaborate heat flows with the volumetric effects of gas radiation and surfaces effects of particle radiation. Such a flow exerts an important influence in the entire mechanism of transport of matter, impulse and heat in the channel and its surroundings. High intensity impulse transfer in the channel results in high gradients of transversal velocities in the cross-section plane.

In straight horizontal channels with non-circular cross-section, a special flow phenomenon occurs, beside the main flow along the channel, during a developed turbulent flow – secondary flows in the cross-section plane of the channel. It is a known fact that, in the channels of arbitrary cross-sections and shapes in both laminar and turbulent flow mode, a secondary flow in the plane perpendicular to the main flow occurs, due to centrifugal forces (curved channels, different heating load, *etc.*) – Prandtl's secondary flow of the first kind. However, in completely straight channels with a square cross-section, and only in the developed turbulent flow mode, a secondary flow is induced in the cross-section of the channel known as Prandtl's secondary flow of the second kind. The secondary flow is a result of transversal gradients of primarily shear stresses in the area of vertices of the channels and produces increased shear stresses towards the vertices of the channel and significantly influences on the intensity of heat transfer from the fluid to the wall of the channel and *vice versa*.

Gas-particle multiphase flow, which may involve a solid or liquid particle, is a significant phenomenon in natural and industrial engineering, such as aerospace, modern chemical industry, energy, metallurgy, material, and environmental protection. Solving gas-particle multiphase flow problems for typical applications are highly important. These applications include burning and flow of metal particles in a solid rocket motor, fluidization in chemical engineering, extraction and utilization of coal, oil, and natural gas for energy, nanoscale manufacturing process, micro-chemical engineering, manufacture of electronic devices, and control of biological metabolism. However, the internal rules and mechanisms of gas and particles are difficult to establish because of the diversity and complexity of problems involved. Numerical simulation has become a powerful tool for examining the characteristics of gas-particle multiphase flow because of the remarkable development in computer technology. Three models, namely, Euler-Euler two-fluid model (TFM), Euler-Lagrange discrete particle model (DPM), and Lagrange-Lagrange pseudo-particle model, are widely used in these numerical simulations.

The Euler–Lagrange DPM has been developed to overcome the limitations of TFM, especially the inability of the latter to trace the path of individual particles. The mechanism of particle–particle collisions can be described by either soft-sphere or hard-sphere model. The soft-sphere model or discrete element model, which was first published in the open literature, is the granular dynamics simulation technique proposed by Cundall and Strack [1]. Then, the contact forces could be calculated from the deformation history of the contact using a contact force scheme. A two-dimensional (2D) soft-sphere approach has been subsequently applied to gas-fluidized beds [2], spouted-fluidized beds [3] and the segregation processes of a binary mixture [4], and this model has been extended to three dimensions by considering the particle motion. In the hard-sphere approach, the interactions between particles are assumed to be pair-wise additive and instantaneous. Campbell and Brennen [5] first reported on hard-sphere discrete particle simulation to study granular systems. The coupling of DPM with a computational fluid dynamics approach for gas-solid two-phase flow was first reported by Hoomans *et al*. [6]. This model has been further used in connection to the kinetic theory of granular flow (KTGF) [7], high-pressure fluidization [8], and circulating fluidized beds [9]. In contrast to the continuum descriptions for the particle phase, DPM can easily describe particle motions,

including particle rotations, and particle-particle collisions, without limiting the number of particles, sizes, and densities. Tanaka et al. [10] introduced DSMC (The direct simulation Monte Carlo) to calculate the particle collisions for a large number of particles in gas–solid flows. Numerical simulations have been performed for a dispersed gas–solid flow in vertical channel [11] and fluidized beds with DSMC method. DSMC has lower computational cost than the hard-sphere and soft-sphere models and is suitable for large-scale simulations. However, details of the particle motion cannot be obtained by the DSMC, and a reasonable sampling number and excellent random number generator are necessary.

A modified model for prediction of erosion rate in pipe flows is presented in [12], based on the simulation of fluid fluctuating velocities with discrete random walk model. Turbulence modulation of gas-solid flow in horizontal pipe is investigated numerically using a four-way coupled Eulerian-Lagrangian approach. The particle impingement angle and impact velocity are evaluated and used for predicting the erosion rate by the available and newly developed models. A modified model for erosion was developed that accounts for the effect of particle size to simulate the wall impact velocity caused by fluid turbulence. The pneumatic conveying of spherical particles in horizontal channel with rectangular cross-section is numerically simulated and presented in [13]. An Eulerian-Eulerian granular phase model is presented in [14] which is extended with Eulerian-Lagrangian discrete phase approaches for rapid granular flows, with the ability to handle poly-dispersed dilute and dense particle-laden flows. Their modification includes the implementation of a new polydispersed drag law and of new boundary conditions distinguishing between sliding and non-sliding particle-wall collisions. Their hybrid model provides substantial savings in terms of computational effort and cost while maintaining satisfactory simulation quality.

Numerical methods represent one of the basic tools of contemporary engineering practice and are used for solving different problems in all fields of the science. The paper employs a full Reynolds stress model of turbulence, which implies that each of the components of Reynolds stress is calculated from its own transport differential equation. These equations are not exact conservation equations but modeled ones [15]. The basic principle used to obtain these equations is to keep correlation of the second order in their original form and members which contain correlations of the third and higher order, of the same or different physical quantities, model with the gradient method, in other words, they are expressed with the gradient of the known physical quantities and model constants.

Physical model

In the basis of all processes of the transport of mater, momentum and heat, the most influential factor and the cause of main difficulties in explaining this phenomenon is turbulence. Turbulence is by its nature a non-stationary, non-linear, irreversible, stochastic, and 3-D phenomenon. The occurrence of the secondary flow in non-circular horizontal channels is a result of turbulent flow mode. The generation of the secondary flow of the second kind depends, above all, on the turbulent fluctuations of the velocity field, where the existence of gradients of Reynolds stresses promotes the secondary fluid flow [16, 17]. The paper considers a fully developed turbulent mode, which assumes that velocity profiles, in other words velocities in the cross-section stabilized in the straight horizontal channel of a square cross-section with walls loaded by uniform turbulent flux.

Systems of fluids with solid particles, in other words, two-phase flows are characterized by a complex of large number interconnected complex phenomena which are a consequence of mutual influence between the phases. In the consideration of such flows with a mu-

tual activity between the phases, the modeling of such flows requires a combined approach to solving the flow field. The gas-flow is solved by applying the Euler approach – the concept of continuum, while the solid phase is solved by applying the Lagrange approach – the concept of tracking the particle trajectories. The interphase interaction of the gas and the solid phase is obtained through an iterative task-solving procedure. In the first step, at the beginning of the integration of conservation equations, the gas phase without the presence of interphase members is solved. In the second step, after a certain number of iterations, the obtained field of the gas-flow is *frozen* and solid particles are *fired* through it. Based on particle trajectories obtained in this way, the interphase members of the solid and gas phase are determined. In the third step, trajectories of solid particles are *frozen* and gas phase flow field is solved again, but this time with the obtained interphase members from the previous step of iteration. If the solution convergence is not achieved, steps two and three are successively repeated until the set criterion of solution convergence is obtained.

For defining the mathematical model of the gas phase, the following assumptions are adopted: the flow is stationary, 3-D, incompressible, isothermal, and chemically inert. To define a mathematical model of the solid phase, the following assumptions are adopted: particles are of various dimensions, particles do not change their mass while travelling through the channel, particles have a constant temperature through the channel, the influence of particle collisions is neglected, particles lose a certain level of impulse upon hitting the channel walls and internal obstacles, particles move stochastically, that is, the turbulent flow field of the gas-flow modulates the deterministic trajectories of particles that are obtained from the averaged values of the gas-flow velocities.

Mathematical model of gas phase

The mathematical model is formed for a 3-D fully developed turbulent flow in a straight horizontal channel with a square cross-section. It is assumed that the turbulent flow is stationary and incompressible, where the channel walls have a constant temperature, which is different from the temperature of the environment. Neglecting the volumetric forces of gravity, the general equation of conservation of impulse, matter and energy for the gas phase corresponds to the equation of field conservation for a single-phase flow, with the addition of the interphase member, and it has the following form [18, 19]:

$$\frac{\partial}{\partial t}(\rho\Phi)+U_j\frac{\partial}{\partial x_j}(\rho\Phi)-\frac{\partial}{\partial x_j}\left(\Gamma_\Phi\frac{\partial\Phi}{\partial x_j}\right)=S_\Phi+S_\Phi^{IF} \tag{1}$$

On the basis of the adopted assumptions of the physical model, the averaged equations of conservation of matter, impulse and heat have the following forms:

– the continuity equation

$$\frac{\partial U_j}{\partial x_j}=0 \tag{2}$$

– the equation of motion

$$U_j\frac{\partial U_i}{\partial x_j}-\frac{\partial}{\partial x_j}\left(\nu\frac{\partial U_i}{\partial x_j}\right)=-\frac{1}{\rho}\frac{\partial P}{\partial x_j}-\frac{\partial\overline{u_iu_j}}{\partial x_j}+S_{U_i}^{IF} \tag{3}$$

– the energy equation

$$U_j \frac{\partial T}{\partial x_j} - \frac{\partial}{\partial x_j}\left(a \frac{\partial T}{\partial x_j} \right) = -\frac{\partial \theta u_j}{\partial x_j} \tag{4}$$

Model of Reynolds' stresses

The starting point to form the stress model of turbulence is a transport equation that defines the dynamic of Reynolds' stresses [20]. The tress model of turbulence assumes simultaneous solutions of the transport equation that defines the dynamic of Reynolds' stresses and the motion equation in Reynolds' averaged form. However, the exact form can treat only particular components of the transport equation for Reynolds' stresses, while the rest of the components of the transport equation are correlations that need to be modeled in the function of available dependently variable values [18, 21].The dependently variable values that are available, for which the transport equations are solved, in the stress model are: averaged velocity, U_i, tensor of turbulent stresses, $\rho\overline{u_i u_j}$, and the velocity of dissipation of turbulent kinetic energy: $\varepsilon = \nu(\partial u_i / \partial x_k)^2$, which, as a phenomenon, is related to for the smallest vortex current, but which depends primarily on energy dominating vortex, and therefore it can be used as a variable that defines the size of this vortex.

The modeled forms of the components in the transport equation which defines the dynamics of Reynolds' stresses [20], lead to the closed form of the transport equation for Reynolds' stresses:

$$U_k \frac{\partial \overline{u_i u_j}}{\partial x_k} = \frac{\partial}{\partial x_k}\left(C_g' \frac{k}{\varepsilon} \overline{u_k u_n} \frac{\partial \overline{u_i u_j}}{\partial x_n} \right) + P_{ij} + \Phi_{ij,1} + \Phi_{ij,2} + \Phi_{ij,z} - \frac{2}{3}\delta_{ij}\varepsilon \tag{5}$$

where

$$P_{ij} = -\overline{u_i u_k}\frac{\partial U_j}{\partial x_k} - \overline{u_j u_k}\frac{\partial U_i}{\partial x_k}, \quad \Phi_{ij} = -C_1 \frac{\varepsilon}{k}\left(\overline{u_i u_j} - \frac{2}{3}\delta_{ij} k \right), \quad D_{ij} = -u_i u_k \frac{\partial U_k}{\partial x_j} - u_j u_k \frac{\partial U_k}{\partial x_j}$$

$$\Phi_{ij,2} = -\alpha\left(P_{ij} - \frac{2}{3}\delta_{ij} P \right) - \beta k \left(\frac{\partial U_i}{\partial x_j} + \frac{\partial U_j}{\partial x_i} \right) - \gamma\left(D_{ij} - \frac{2}{3}\delta_{ij} P \right)$$

$$\Phi_{ij,z1} = C_{z1}\left(\overline{u_k u_m}\delta_{ij} n_k n_m - \frac{3}{2}\overline{u_k u_i} n_k n_j - \frac{3}{2}\overline{u_k u_j} n_k n_i \right) f_z \frac{k}{\varepsilon}$$

$$\Phi_{ij,z2} = C_{z2}\left(\Phi_{km,2}\delta_{ij} n_k n_m - \frac{3}{2}\Phi_{ki,2} n_k n_j - \frac{3}{2}\Phi_{kj,2} n_k n_i \right) f_z$$

$$P = -\overline{u_i u_j}\frac{\partial U_i}{\partial x_j}, \quad f_z = \frac{C_\mu^{0.75} k^{1.5}}{0.417\varepsilon}\frac{1}{x_{nz}}, \quad \Phi_{ij,z} = \Phi_{ij,z1} + \Phi_{ij,z2}$$

The closing of the stress model for Reynolds' stresses, eq. (5), is performed by an additional transport differential equation for the dissipation of turbulent kinetic energy, so that the dissipation of the kinetic energy of turbulence, ε, appears as a new added variable which is determined from its own transport equation:

$$U_k \frac{\partial \varepsilon}{\partial x_k} = \frac{\partial}{\partial x_k}\left(C_\varepsilon \frac{k}{\varepsilon} \overline{u_k u_j} \frac{\partial \varepsilon}{\partial x_j} \right) + \frac{\varepsilon}{k}(C_{\varepsilon 1} P - C_{\varepsilon 2}\varepsilon) \tag{6}$$

The empirical coefficients for the turbulence model for Reynolds' stresses in eqs. (5) and (6) are given in tab. 1.

Table 1

C'_g	C_1	C_2	C_{z1}	C_{z2}	C_μ	C_ε	$C_{\varepsilon 1}$	$C_{\varepsilon 2}$
0.21	1.50	0.40	0.50	0.06	0.09	0.15	1.44	1.90

Model of turbulent temperature fluxes

A transport differential equation for turbulent temperature fluxes [18] also cannot be solved in its exact form, but it needs to be modeled, like in the case of the transport equation for Reynolds' stresses. By modeling the components in the transport equation for turbulent temperature fluxes, the closed form of the transport equation is obtained:

$$U_k \frac{\partial \overline{\theta u_i}}{\partial x_k} = \frac{\partial}{\partial x_k}\left(C_\theta \frac{k}{\varepsilon} \overline{u_k u_j} \frac{\partial \overline{\theta u_i}}{\partial x_j} \right) + P_{\theta i} + \Phi_{\theta i} + \Phi_{\theta i,z} + \varepsilon_{\theta i} \tag{7}$$

where

$$P_{\theta i} = -\overline{u_k u_i} \frac{\partial T}{\partial x_k} - \overline{\theta u_k} \frac{\partial U_i}{\partial x_k}, \quad \Phi_{\theta i} = -C_{\theta 1} \frac{\varepsilon}{k} \overline{\theta u_i} + C_{\theta 2} \overline{\theta u_k} \frac{\partial U_i}{\partial x_k}, \quad \Phi_{\theta i,z} = -C_{\theta 1 z} \frac{\varepsilon}{k} \overline{\theta u_k} n_i n_k f_z$$

Table 2

C_θ	$C_{\theta 1}$	$C_{\theta 2}$	$C_{\theta z1}$
0.11	2.45	0.66	0.80

The empirical coefficients of the model of turbulent temperature fluxes in eq. (7) are given in tab. 2.

Mathematical model of the solid phase

In the vast majority of technical processes found in the engineering practice, the presence of solid particles in flows greatly complicates the problem, both because of the need to model the flow of the discrete phase and due to the interaction of the phases. The presence of particles creates aerodynamic resistances that condition the change in the momentum of both phases. The mathematical model of the solid phase is based on the Lagrange concept of task solution, which is closer to the physical reality and provides more realistic image and more reliable predictions of the motion of solid particles in the turbulent flow of fluids by offering more information (trajectory, time spent in certain space).

The position of solid particles is determined by solving the equation of motion for each group of particles:

$$\frac{\mathrm{d}x_\mathrm{p}}{\mathrm{d}t} = \vec{\mathrm{U}}_\mathrm{p} \tag{8}$$

The current velocity of solid particles is determined from the equation of the solid phase impulse:

$$m_{\mathrm{p}} \frac{\mathrm{d}\vec{\mathrm{U}}_{\mathrm{p}}}{\mathrm{d}t} = \Re_{\mathrm{p}}(\vec{\mathrm{U}} - \vec{\mathrm{U}}_{\mathrm{p}}) + m_{\mathrm{p}} b\mathrm{g} - V_{\mathrm{p}} \nabla P \tag{9}$$

The first member on the right side of the (9) represents the force of resistance to the relative motion of particles in relation to the gas phase and it is the dominant force that causes the motion of solid particles in the direction of the channel axis. The second member represents the force of gravity, and the third member represents the force of buoyancy. The forces of gravity and buoyancy are perpendicular to the direction of motion of solid particles, that is, to the direction of the force of resistance to the relative motion, but are of opposite sense of direction, therefore, when solving the set task it is assumed that their effects on the solid particle are in balance. This means that the solid particles are affected only by the force of resistance to relative motion which causes the motion of the solid particles. Furthermore, in the process of solving this task, the following forces are neglected: the force due to the increase in the pressure gradient, Basset, Saffman, and Magnus forces.

In eq. (9) $\Re_{\mathrm{p}}$ represents a function of the resistance of a solid particle and it is determined by:

$$\Re_{\mathrm{p}} = 0.5 \rho A_{\mathrm{p}} C_D \left| \vec{\mathrm{U}} - \vec{\mathrm{U}}_{\mathrm{p}} \right| \tag{10}$$

where C_D is the coefficient of resistance, for spherical solid particles of the transported material and Reynolds number, $\mathrm{Re} < 10^5$, is defined by:

$$C_D = \frac{24}{\mathrm{Re}}(1 + 0.15\,\mathrm{Re}^{0,687}) + \frac{0.42}{1 + 4.25 \cdot 10^4\,\mathrm{Re}^{-1,16}} \tag{11}$$

Integrating the momentum equation of solid particles, eq. (9), is performed in the second iterative step, in the way that Lagrange time step of integration is determined firs, then the motion of particles is started based on its initial and border conditions. Thereafter, characteristics and interphase components of the particle are determined for each new position of the particle.

Lagrange time step of integration is determined based on:

$$\Delta t_{\mathrm{L}} = \max\left[t_0, \min(t_1, t_2, t_3)\right] \tag{12}$$

where t_0 is the minimum time step which is adapted arbitrarily, and its value is not smaller than 10^{-7} seconds, t_1 – the time step obtained when the minimum time of the passage of the particle through a numerical cell is divided by the minimum number of Lagrange's steps that is not bigger than 10, t_2 – the time of relaxation of impulses, which can be determined by solving the momentum equation in the form: $\mathrm{d}\vec{\mathrm{U}}_{\mathrm{p}} \big/ \mathrm{d}t = A - B\vec{\mathrm{U}}_{\mathrm{p}}$, and t_3 – the maximum time step that is bigger than t_1 and t_2 .

Lagrange time step can be reduced after determination of the next particle position, in a way that the particles path are not allowed to be bigger than the numerical grid cell. If the current time step is so big so that the new computed particle position is bigger than distance between grid nodes, the time step is decreased in order to time integration to be carried out for all numerical grid cells. The Lagrangian time step is reduced in boundary grid cells.

After Lagrange time step, ∇t_{L}, is determined, *motion* of particles is started by integrating trajectory equations of the particle (8). The integral of this equation is:

$$x_{\mathrm{p}}^n = x_{\mathrm{p}}^0 + \vec{\mathrm{U}}_{\mathrm{p}}^0 \Delta t_{\mathrm{L}} \tag{13}$$

where n is the marked value of a position vector of the particle at the end of the time step, and 0 – the value of a position vector at the beginning of the time step.

The characteristics of the solid particles are determined by solving equations of impulse of particles, eq. (9), which can be written in the general form:

$$\frac{\mathrm{d}\tilde{X}}{\mathrm{d}t} = A - B\tilde{X} \tag{14}$$

where $\tilde{X}$ is the corresponding current variable of the solid particle (for instance, impulse, mass, enthalpy) and A and B are the constants [22].

The basic problem when considering two-phase turbulent flows of the gas-solid particles type is related to the treatment of the mutual exchange of the momentum, energy and mass between the phases, because the particles go from one vortex to another. When modeling the two-phase turbulent flow, the presence of disperse phase cases the occurrence of additional sources of momentum, energy and mass in equations of the gas phase. The basic approach to determining the interphase components of interaction is based on the division of the flow field into numerical cells and taking each cell as a control volume.

The mathematical model of the continual phase is based on the models developed for a pure fluid-air along with the correction due to the presence of the solids. Namely, when a particle goes through the entire numerical cell, the interphase interactions of changing the impulse, energy or mass occur. This means that, if a particle moves with a speed larger than the surroundings, *i. e.* the gas phase, the particle slows down because of the interactions of phases, *i. e.* the velocity of the particle will decrease while the velocity of the gas phase in the surroundings of the solid particle will increase. Also, if a particle moves with a speed smaller than the speed of its surroundings, the velocity of the particle increases because the interactions between phases, while the velocity of the gas phase in the surrounding decreases. Mutual influences, *i. e.* interactions between phases are defined by interphase components. These interphase components need to be added to the equation of motion of the gas phase, so they need to be appropriately determined. The interphase components of interactions describe the changes of momentum of particles of the transported material, *i. e.* the change in the momentum of the gas phase due to the presence of solid particles. The interphase component of the interaction in eq. (3) represents in fact the force of resistance to the motion of the solid particle in the air-flow, *i. e.* the force of resistance to the flow of the fluid surrounding the solid particle, which is of the same intensity and the trajectory but of the opposite direction than the force of resistance reaction caused by the motion of the particle [23]. When modeling, the influences of forces perpendicular to the trajectory of solid particles are not considered, *i. e.* it is assumed that these forces are balanced. This means that the mutual influence between phases is actually given by the intensity of forces acting in the direction of solid particles' motion, and the interphase component of the interaction is determined by integrating equations of particle motion:

$$m_{\mathrm{p}} \frac{\mathrm{d}\vec{\mathrm{U}}_{\mathrm{p}}}{\mathrm{d}t} = S_{U_i}^{IF} \tag{15}$$

Integration of eq. (15) is performed for each numerical cell, taking into consideration Lagrange time step, in order not to skip cells, *i. e.* in order to perform integration for each numerical cell, which means for the entire cross-section of the channel. The interphase components of the interaction between phases which occur in the equation of the gas phase motion (3) are equal to the change of the impulse of motion of solid particles for each numerical cell

and describe the change of the momentum of the gas phase due to the presence of solid particles in it, and they are determined in the following way:

$$S_{U_i}^{IF} = \frac{\pi}{6}\sum\eta\left[\rho_{\mathrm{p}}^{0}\,\vec{\mathrm{U}}_{\mathrm{p},i}^{0}\left(D_{\mathrm{p}}^{0}\right)^{3} - \rho_{\mathrm{p}}^{n}\,\vec{\mathrm{U}}_{\mathrm{p},i}^{n}\left(D_{\mathrm{p}}^{n}\right)^{3}\right] \tag{16}$$

Numerical model

The basic problem considering two-phase flow of gas-solid particle type is based on the change of the momentum, energy, and mass of particles, *i. e.* transported material when they pass through a certain segment of the flow field, whereby the changes have to remain in the gas phase. A change in the momentum of particles during the passing through the observed numerical control volume is taken as the source or sink of the momentum of the continuous – gas phase. In this case, the mathematical model of the gas phase is set for the single-phase flow with the correction related to the presence of solid particles.

In order to solve the set problem, a fully developed two-phase air-solid particle turbulent flow in a straight channel with a square cross-section, and with the dimensions of the sides of 200 mm is observed. So as to form the mode of the fully developed turbulent flow with constant velocities, thus inducing the secondary flow known as Prandtl's secondary flow of the second kind, an 80 D_h long channel is taken, which amounts to 18 m, fig. 1.

The numerical grid along the cross-section is not uniform, which leads to numerical cells being of various sizes, fig. 2. The numerical cells in the central part of the channel are less densely packed and have larger surfaces, while the cells in the vicinity of the channel walls and vertices are denser and have smaller surfaces. The mass-flow of solid particles through the cross-section of the channel at its entrance is given as a partial flow in the numerical cells, proportional to the surface of the cells. Since the numerical cells are of different surfaces, that is, the cells in the vicinity of the channel walls and vertices have smaller surfaces, the mass-flows of particles in them are smaller as well, contrary to the bigger numerical cells located in the middle part of the channel with larger mass-flows within them.

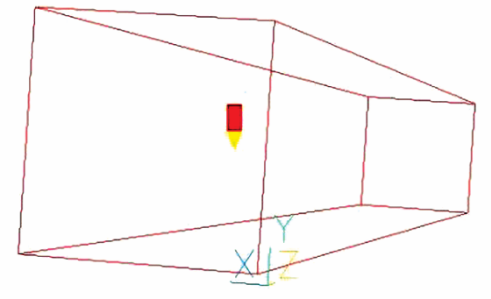

Figure 1. The shape of the channel

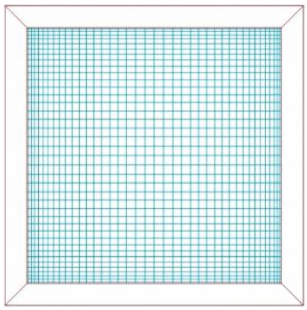

Figure 2. The numerical grid

In this way, when the entire cross-section of the channel is observed, a balanced distribution of transported solid particles along the entire cross-section is obtained. During the simulations, the influence of the fineness of the numerical grid was examined on three different numerical grids (30 × 30 × 180, 35 × 35 × 180, and 40 × 40 × 180), and Euclidian norm for bulk dimensionless velocity between these grids was $\varepsilon = 0.0035$ and $\varepsilon = 0.0014$, respectively for dimensionless time step $\Delta t = 0.005$. The paper presents the results of the highest

resolution of the numerical grid above which the fineness of the grid did not affect the obtained results, with the number of cells in $x^1 \equiv x$, $x^2 \equiv y$, and $x^3 \equiv z$-directions, respectively, $40 \times 40 \times 180$. Figure 2 shows the positions of the transported solid particles, the velocities of which along the channel are given in figs. 6(d), 7(d), and 8(d).

Mechanisms which lead to the occurrence of secondary flows of both the first and the second order are different in turbulent flows. The influence of Prandtl's secondary flow of the second order, regardless of its value, cannot be neglected, especially not in the cases of two-phase flow of gas-solid particles type, where solid particles of the transported material are relatively small in diameter, *i. e.* in two-phase flow with a high Stokes number. In order to notice the effects of the secondary flow of the second type in the cross-section of the observed channel, three cases of simulation of the two-phase flow of gas-solid particles type are considered, where the transporting fluid has always been air of the same characteristics, while particles of quartz, ash and flour have been used as the transported material.

Firstly, solid particles of quartz of $D_p = 0.5$ mm in diameter and $\rho_p = 2500$ kg/m^3 in density are used as the transported material. In order to initiate the motion of the transported material, *i. e.* the solid particles an initial velocity at the entrance of the channel, which corresponded to the suspension velocity of the particles, which amounts to $U_p = V_p = 0$, $W_p = 2.8$ m/s for quartz. Ash was used the following transported material in the model, with $D_p = 0.14$ mm in diameter and $\rho_p = 1800$ kg/m^3 in density with the suspension velocity of $U_p = V_p = 0$, $W_p = 0.36$ m/s, and flour of $D_p = 0.20$ mm in diameter, $\rho_p = 1410$ kg/m^3 in density and the suspension velocity of $U_p = V_p = 0$, $W_p = 1.2\text{-}1.5$ m/s. To form the mathematical model of the transported ash and flour particles, so as to reduce the iteration procedure, the same initial velocity at the entrance of the channel was adopted as with quartz $U_p = V_p = 0$, $W_p = 2.8$ m/s. When forming the mathematical model, the transported particles are equally distributed at the entrance of the channel across the entire cross-section of the channel. So as to model the flow and to notice the behavior of the transported material, six groups of particles were chosen, which were equally distributed in the cross-section of the channel along the x- and y-axis, figs. 6(b), 7(b), and 8(b). To record the behavior of the transported material, six groups of particles were selected and distributed along the x- and y-axis. The boundary condition at the entrance cross-section of the channel for diameter, density, mass flow, and concentration distribution for particles (solid phase) has been given in tab. 3.

The total mass-flow through the cross-section of the channel in numerical cells was given as a partial flow proportional to the size of the cells. In other words, the mass-flows of the solid particles were given in such a way that smaller mass-flow was given to the cells of a smaller size, and bigger mass-flow through numerical cells of a bigger size. In addition to defining the initial velocities of the transported particles of quartz, it is needed to define the velocity of the flow of transporting air at the entrance, which amounts to $W = 12\text{-}22$ m/s for transporting quartz particles, $W = 12\text{-}20$ m/s for ash particles, and approximately $W = 20$ m/s for flour particles [23]. In this paper, the adopted air velocity at the entrance was $W = 22$ m/s, with the pressure of $p = 1$ bar and $\rho = 1.2$ kg/m^3 in density for all three models of turbulent two-phase flow.

To simulate the two-phase turbulent flow, the isothermal, stationary and 3-D flow of the transporting air was observed, and it is assumed that the mass and the temperature of the solid particles, which move stochastically along the channel, do not change during the transport process and the influence of mutual collisions of particles, as well as collisions of the particles with the walls are neglected. So as to solve the mathematical model, it is assumed that the temperature of the channel walls does not change along the channel and that it is different from the temperature of the surroundings.

Table 3. Diameter, density, mass-flow, and the concentration distribution of spheric particles at the entrance cross-section of the channel

						Quartz			Ash			Flour		
X_p [m]	Y_p [m]	Z_p [m]	U_p [ms^{-1}]	V_p [ms^{-1}]	W_p [ms^{-1}]	D [m]	ρ [kgm^{-3}]	$\dot{m}$ [kgs^{-1}]	D [m]	ρ [kgm^{-3}]	$\dot{m}$ [kgs^{-1}]	D [m]	ρ [kgm^{-3}]	$\dot{m}$ [kgs^{-1}]
Group 1														
0.01412	0.01412	0	0	0	2.8	5.00E-04	2500	6.85E-02	1.40E-04	1800	6.85E-02	2.00E-04	1410	6.85E-02
0.01412	0.03913	0	0	0	2.8	5.00E-04	2500	8.84E-02	1.40E-04	1800	8.84E-02	2.00E-04	1410	8.84E-02
0.01412	0.07663	0	0	0	2.8	5.00E-04	2500	1.05E-01	1.40E-04	1800	1.05E-01	2.00E-04	1410	1.05E-01
0.01412	0.1234	0	0	0	2.8	5.00E-04	2500	1.05E-01	1.40E-04	1800	1.05E-01	2.00E-04	1410	1.05E-01
0.01412	0.1609	0	0	0	2.8	5.00E-04	2500	8.84E-02	1.40E-04	1800	8.84E-02	2.00E-04	1410	8.84E-02
0.01412	0.1859	0	0	0	2.8	5.00E-04	2500	6.85E-02	1.40E-04	1800	6.85E-02	2.00E-04	1410	6.85E-02
0.01412	0.01412	0	0	0	2.8	5.00E-04	2500	6.85E-02	1.40E-04	1800	6.85E-02	2.00E-04	1410	6.85E-02
Group 2														
0.03913	0.01412	0	0	0	2.8	5.00E-04	2500	8.86E-02	1.40E-04	1800	8.86E-02	2.00E-04	1410	8.86E-02
0.03913	0.03913	0	0	0	2.8	5.00E-04	2500	1.15E-01	1.40E-04	1800	1.15E-01	2.00E-04	1410	1.15E-01
0.03913	0.07663	0	0	0	2.8	5.00E-04	2500	1.36E-01	1.40E-04	1800	1.36E-01	2.00E-04	1410	1.36E-01
0.03913	0.1234	0	0	0	2.8	5.00E-04	2500	1.36E-01	1.40E-04	1800	1.36E-01	2.00E-04	1410	1.36E-01
0.03913	0.1609	0	0	0	2.8	5.00E-04	2500	1.15E-01	1.40E-04	1800	1.15E-01	2.00E-04	1410	1.15E-01
0.03913	0.1859	0	0	0	2.8	5.00E-04	2500	8.86E-02	1.40E-04	1800	8.86E-02	2.00E-04	1410	8.86E-02
Group 3														
0.07663	0.01412	0	0	0	2.8	5.00E-04	2500	1.05E-01	1.40E-04	1800	1.05E-01	2.00E-04	1410	1.05E-01
0.07663	0.03913	0	0	0	2.8	5.00E-04	2500	1.35E-01	1.40E-04	1800	1.35E-01	2.00E-04	1410	1.35E-01
0.07663	0.07663	0	0	0	2.8	5.00E-04	2500	1.61E-01	1.40E-04	1800	1.61E-01	2.00E-04	1410	1.61E-01
0.07663	0.1234	0	0	0	2.8	5.00E-04	2500	1.61E-01	1.40E-04	1800	1.61E-01	2.00E-04	1410	1.61E-01
0.07663	0.1609	0	0	0	2.8	5.00E-04	2500	1.35E-01	1.40E-04	1800	1.35E-01	2.00E-04	1410	1.35E-01
0.07663	0.1859	0	0	0	2.8	5.00E-04	2500	1.05E-01	1.40E-04	1800	1.05E-01	2.00E-04	1410	1.05E-01
Group 4														
0.1234	0.01412	0	0	0	2.8	5.00E-04	2500	1.05E-01	1.40E-04	1800	1.05E-01	2.00E-04	1410	1.05E-01
0.1234	0.03913	0	0	0	2.8	5.00E-04	2500	1.35E-01	1.40E-04	1800	1.35E-01	2.00E-04	1410	1.35E-01
0.1234	0.07663	0	0	0	2.8	5.00E-04	2500	1.61E-01	1.40E-04	1800	1.61E-01	2.00E-04	1410	1.61E-01
0.1234	0.1234	0	0	0	2.8	5.00E-04	2500	1.61E-01	1.40E-04	1800	1.61E-01	2.00E-04	1410	1.61E-01
0.1234	0.1609	0	0	0	2.8	5.00E-04	2500	1.35E-01	1.40E-04	1800	1.35E-01	2.00E-04	1410	1.35E-01
0.1234	0.1859	0	0	0	2.8	5.00E-04	2500	1.05E-01	1.40E-04	1800	1.05E-01	2.00E-04	1410	1.05E-01
Group 5														
0.1609	0.01412	0	0	0	2.8	5.00E-04	2500	8.86E-02	1.40E-04	1800	8.86E-02	2.00E-04	1410	8.86E-02
0.1609	0.03913	0	0	0	2.8	5.00E-04	2500	1.15E-01	1.40E-04	1800	1.15E-01	2.00E-04	1410	1.15E-01
0.1609	0.07663	0	0	0	2.8	5.00E-04	2500	1.36E-01	1.40E-04	1800	1.36E-01	2.00E-04	1410	1.36E-01
0.1609	0.1234	0	0	0	2.8	5.00E-04	2500	1.36E-01	1.40E-04	1800	1.36E-01	2.00E-04	1410	1.36E-01
0.1609	0.1609	0	0	0	2.8	5.00E-04	2500	1.15E-01	1.40E-04	1800	1.15E-01	2.00E-04	1410	1.15E-01
0.1609	0.1859	0	0	0	2.8	5.00E-04	2500	8.86E-02	1.40E-04	1800	8.86E-02	2.00E-04	1410	8.86E-02
Group 6														
0.1859	0.01412	0	0	0	2.8	5.00E-04	2500	6.85E-02	1.40E-04	1800	6.85E-02	2.00E-04	1410	6.85E-02
0.1859	0.03913	0	0	0	2.8	5.00E-04	2500	8.84E-02	1.40E-04	1800	8.84E-02	2.00E-04	1410	8.84E-02
0.1859	0.07663	0	0	0	2.8	5.00E-04	2500	1.05E-01	1.40E-04	1800	1.05E-01	2.00E-04	1410	1.05E-01
0.1859	0.1234	0	0	0	2.8	5.00E-04	2500	1.05E-01	1.40E-04	1800	1.05E-01	2.00E-04	1410	1.05E-01
0.1859	0.1609	0	0	0	2.8	5.00E-04	2500	8.84E-02	1.40E-04	1800	8.84E-02	2.00E-04	1410	8.84E-02
0.1859	0.1859	0	0	0	2.8	5.00E-04	2500	6.85E-02	1.40E-04	1800	6.85E-02	2.00E-04	1410	6.85E-02

The presence of particles in the turbulent flow complicated the problem, both because of the need to model the discrete phase flow and due to the interaction of the phases. Since this was the case of turbulent flow, the transported material particles were affected by both the averaged and the fluctuating components of forces. The solid particles migrate from one vortex to another, whereby the aerodynamic resistance causes the change of the momentum of both phases. The caused changes of the momentum, energy and mass of the solid particles of the transported material when passing through a certain segment of the flow field remain in the gas phase. The change of the momentum of the particles during the passage through the observed numerical control volume is taken as the source or sink of the momentum of the continuous gas phase. The continuous phase air-flow is treated as a continuum and is solved by applying the Euler approach, the concept of continuum, while the solid phase is solved by applying the Lagrange approach, which can be reduced to tracing their trajectories and changes in the velocity, temperature and mass of the particles along these trajectories. The presence of the solid phase is taken into consideration as a source of sink of momentum in equation for the gas phase. The solution of the mathematical model was performed in the iterative manner until the solution convergence of 0.1% was reached.

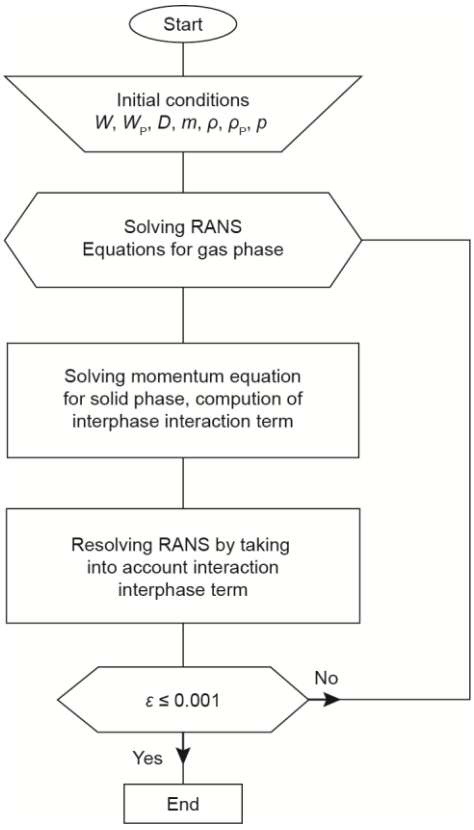

Figure 3. The flowchart of numerical computation

The iterative procedure comprised four successively repeated steps. In the first iterative step only airflow field is considered, and the gas phase conservation equations are calculated as if the dispersed phase were absent. The integration conservation equation of gas phase is carried out as if the existences of solid particles do not have influence on gas phase flow field. The presence of dispersed phase causes the appearance of additional terms in gas phase momentum equation as sink term and as source term in solid phase due to interaction between gas and solid phase. In the second iterative step the computed gas phase flow field is *frozen* with respect to time, and we calculate forces by which gas phase flow field acts on solid particles. In this way in the frozen gas phase flow field, the trajectories of solid particles are computed. On the basis of obtained trajectories of solid particles in such way, the interphase interaction sink term in momentum equation of gas phase and source term in solid phase momentum equation are determined. In the next, third iterative step the gas phase flow field is again calculated but now taking into account the interphase interaction sink term obtained on the basis of calculated trajectories of solid phase which is now temporally frozen. The second and third iterative steps are repeated until the desired solution convergence criterion of 0.1% is achieved. The flowchart of numerical computation is shown in fig. 3.

Results and discussion

The two-phase flow in straight channel of quadratic cross-section has been considered for the validation of turbulence stress model that was used in Po's [24] and Perkins's [25] experiments. Turbulent kinetic energy and Reynolds stress distribution and evolution have been considered normalized with respect to bulk velocity of channel flow. On the basis of obtained diagrams the good correlation (agreement) between experimental and numerical results has been achieved, figs. 4 and 5. For the need of results comparison between mono-phase and two-phase flow, the numerical simulations of mono-phase gas flow and two phase flow have been carried out for the same boundary conditions of gas phase flow but for several different solid particles dispersed in the gas-flow, whereby the mesh density has been kept unaltered. Dominant parameters that influence the secondary flow of second kind are turbulent shear stresses in channel cross-section, and they are chosen as parameters for two-phase flows comparison with different solid particles [22].

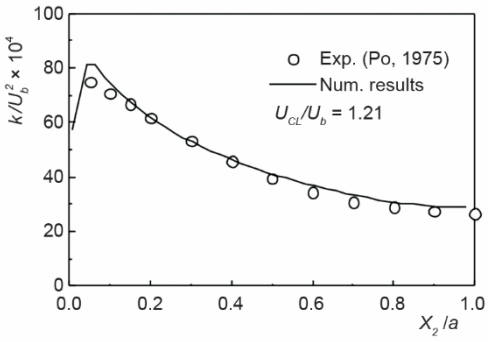

Figure 4. Kinetic energy distribution with respect to x_2-axis

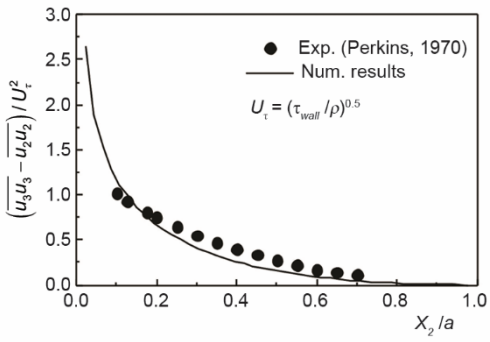

Figure 5. Normal Reynolds stress difference distribution along the x2-axis

In the paper, the full Reynolds' stress model of turbulence is used for solving the two-phase flow. The stress model assumes simultaneously solving the transport equations for the turbulent stresses with the equation for motion in Reynolds' averaged form. Some important pieces of information are lost when the Reynolds' equations are averaged in time, namely, correlations of fluctuation parts of different physical quantities occur, which are modeled in the function of available dependently variable values: averaged velocity, tensor of turbulent stresses, and the speed of dissipation of turbulent kinetic energies, in order to determine the mathematical model. The full Reynolds stress model assumes that each component of Reynolds stress is determined from its own transport differential equation, which is modeled.

To solve the set problem of pneumatic transport, six groups of particles were observed, which were distributed along the x- and y-axis, figs. 6(b), 7(b), and 8(b). In order to begin with solving the mathematical model of two-phase flow, the initial velocity of the solid particles at the entrance of the channel, as well as the velocity of the transporting air is to be set. The initial velocity of the particles is chosen to be the same for all materials W_p = 2,8 m/s, and it corresponds to the suspension velocity of the particles of quartz in the fluid current (air), in order to reduce the duration of the iteration procedure, although the suspension velocities of flour and ash are somewhat smaller. Furthermore, the same value is chosen for the velocity of the transporting air at the entrance of the channel, which amounts to W = 22 m/s. The mathematical model is set to observe the motion of the solid particles of the spherical shape of

the recommended values of equivalent diameter and density. Since the chosen numerical grid is not uniform, *i. e.* the grid contains numerical cells of different sizes, partial mass-flows in the cells are given proportionally to the size of the cells. For the numerical cells in the middle of the channel, where the sizes are larger, the flows are also larger, while the sizes of the cells in the vicinity of the walls of the channels are smaller, and so are the flows.

The formation of the secondary flow of the second order in the straight channel of a non-circular cross-section during the fully developed turbulent flow occurs sue to the existence of the gradients of Reynolds stresses. The dominant parameters that influence the secondary flow of the second kind are the turbulent tangential stresses in the transversal plane of the channel. The turbulent components that contain Reynolds stresses have the dominant role and they have the opposite sign in the transport equation for the component of vorticity perpendicular to the plane of the cross-section. These members express the influence of the turbulent stresses on the production and destruction of the turbulent vorticity. It can be said that the vorticity is larger if the production of the turbulent stresses is larger, if this difference is greater, the secondary flow is more intensive and expressed. The presence of solid particles in the gas phase causes the increase in this difference between components that contain turbulent stresses, thus they result in the more intensive secondary flow.

The two-phase flows are characterized in the general sense by the complex of a large number of mutually related phenomena, which are the consequences of multicomponentness of a mixture. The dispersive phase affects the changes typical for the flow of the carrying fluid – the air and *vice versa*. The presence of the solid phase is taken into consideration though added components that define the interphase sources or sinks of momentum, matter or heat in the equation of conservation of the gas phase. The solid particles of the transported material move because of the action of the force of resistance reaction. Apart from the force of resistance reaction which acts in the direction of the particle motion and causes their motion, the particles are also acted upon by forces perpendicular to their movement direction. The vertical direction is affected by buoyancy and gravitation force. Since it is a turbulent flow, the particles are affected by both averaged and fluctuating components of these forces. The fluctuating components of vertical forces, supported by the action of Magnus and Basset forces, act upon the particles in such a way that they prevent their precipitation in the channel. If these forces are not sufficient to lift the particles in the basic current, *i. e.* if the vertical forces are not balanced, the disturbance of the motion of particles in the channel occurs. In that case, the precipitation of the particles at the bottom of the channel may occur, this can lead to the discontinuation of the transport of materials. In the paper, it is assumed that the forces perpendicular to the motion direction of the particles are balanced.

The performed numerical simulations produced a reliable stress model of turbulence which describes the complex physics of turbulent induction of the secondary flow in the straight channels with non-circular cross-section, as well as the production of adequate interphase members of interaction in the systems of two-phase flow of the gas-solid particles type with a high Stokes number. The motion of particles was traced by the Lagrange method, *i. e.* each particle was traced along its trajectory, with certain assumptions: mutual collisions of particles are neglected and elastic collisions with the channel's walls were assumed. The stress model of turbulence which describes the physics of the turbulent induction of the secondary flow in the straight channels with the non-circular cross-section produced the interphase members of interactions between the gas and dispersive phase, which also defined the influence of the turbulent diffusion of dispersive phase in the system of two-phase flow of the gas-solid particles type.

Figures 6(a), 7(a), and 8(a) show the trajectories of the particles, their distribution at the entrance is given in figs. 6(b), 7(b), and 8(b), and the velocities of the transported solid particles along the channels in figs. 6(d), 7(d), and 8(d), and in the cross-section of the channel –

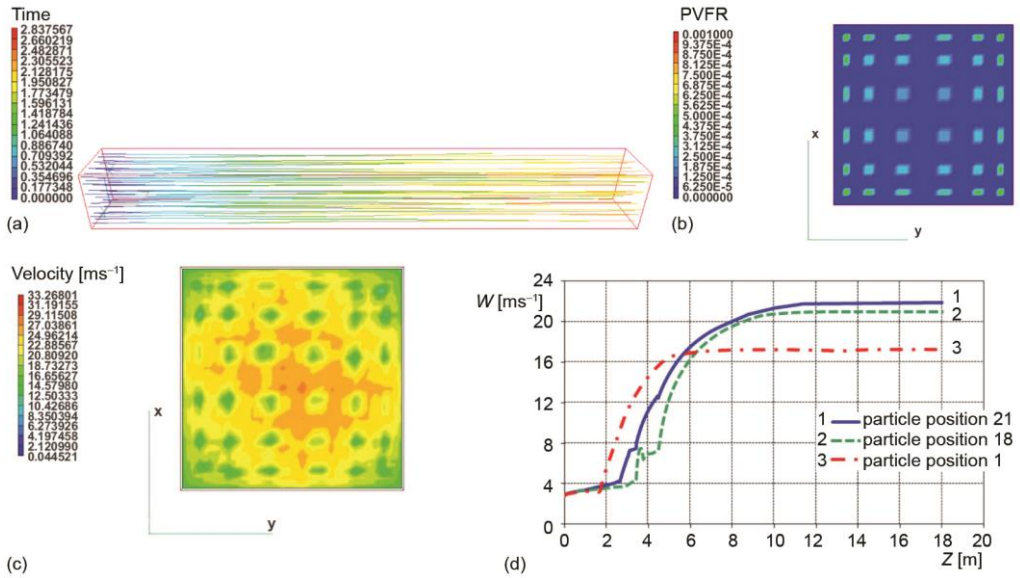

Figure 6. Motion of the quartz particles; (a) trajectory of the particles, (b) distribution of the particles at the entrance, (c) velocity change in the cross-section, (d) velocity change along the channel
(*for color image see journal web site*)

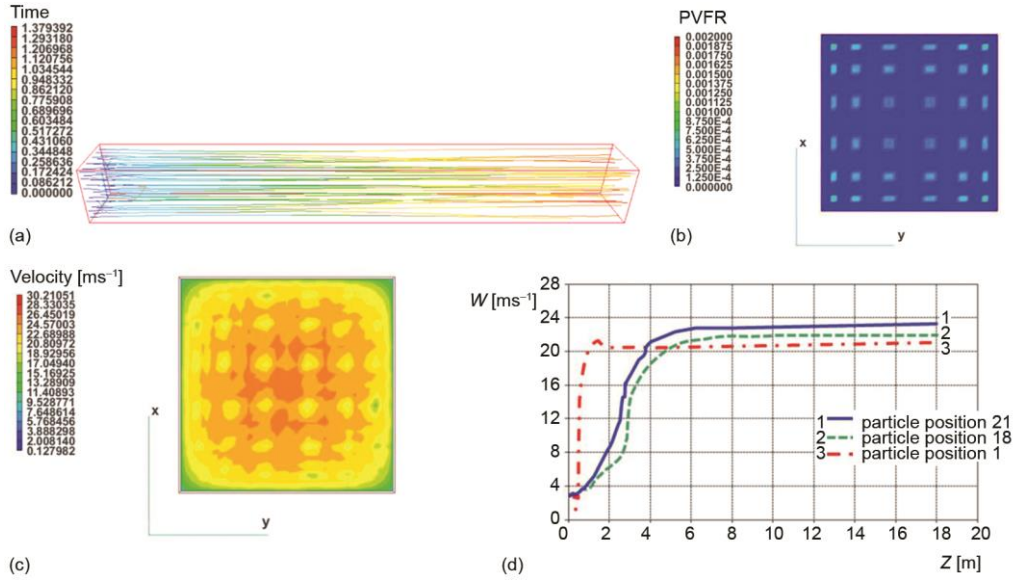

Figure 7. Motion of the ash particles; (a) trajectory of the particles, (b) distribution of the particles at the entrance, (c) velocity change in the cross-section, (d) velocity change along the channel
(*for color image see journal web site*)

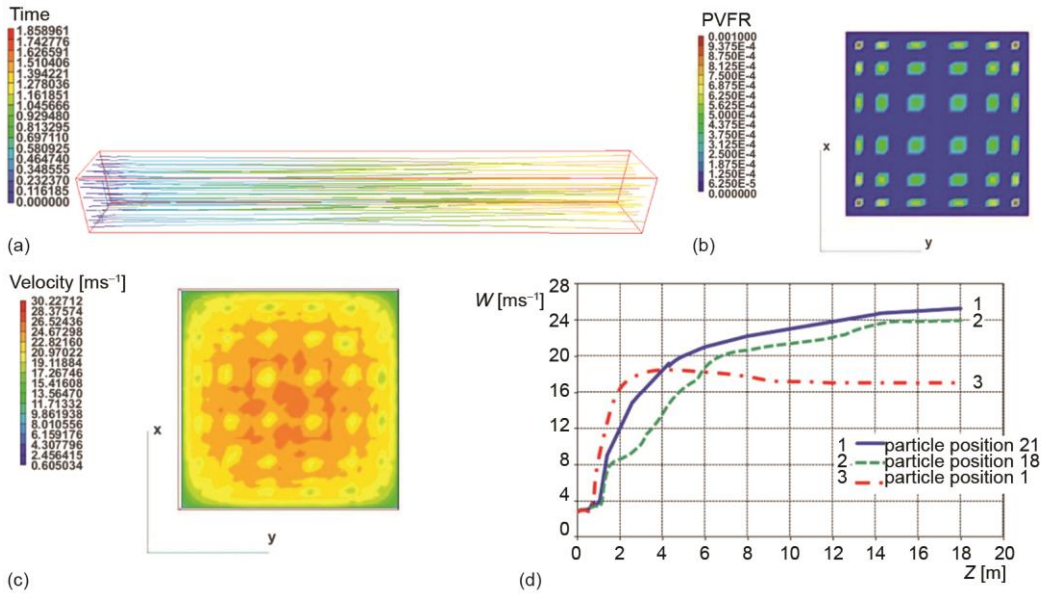

Figure 8. Motion of the flour particles; (a) trajectory of the particles, (b) distribution of the particles at the entrance, (c) velocity change in the cross-section, (d) velocity change along the channel
(*for color image see journal web site*)

figs. 6(c), 7(c), and 8(c). The solid particles fill the entire cross-section of the channel from the entrance to the exit, which allows the transport of materials (particles). Viscous zones caused by the secondary flow directly along the hard wall and in the vertices of the channel affect the turbulent interactions with their damping action, which is clearly seen at the beginning of the channel, when the velocities of the particles are the smallest. Developing of the flow causes the velocities to increase, but mostly in the central area of the channel, where it is the largest full line, closer to the walls, the velocity is smaller, interrupted line, and it is the smallest in the vicinity of the vertices of the channel, with dotted line, figs. 6(d), 7(d), and 8(d).

Conclusions

A fully developed turbulent flow in straight channels with a non-circular cross-section, with the isolated effect of the secondary flow of the second kind was considered. The turbulent transport of the momentum, heat and matter is the main characteristic of the fluid--flow which is seen every day not only in engineering and technical devices, but also in natural flows of water and atmospheric flows. Numerical simulations of transport processes, matter and momentum during the turbulent two-phase flow were performed using the software package PHOENICS 3.3.1, which is based on control volume method. All numerical experiments were conducted for the same initial flow conditions. A correction of the stress model of the turbulence is performed considering the influences of damping-promoting effects of interactions of the gas and solid phase. The full Reynolds stress model of turbulence was used for solving the two-phase flow, and the complete model was used for the turbulent stresses and turbulent temperature fluxes. The obtained stress model of turbulence describes the physics of the turbulent induction of the secondary flow in the straight channels with a non-circular

cross-section and the interphase members of the interactions between gas and solid phase were determined. The conducted numerical simulations provided the distribution of the velocities of transported particles, which shows that no precipitation will occur in the channel and that the desired transport can be realized. A reliable engineering tool was obtained based on a numerical approach to calculations of the complex phenomena of the pneumatic transport in the channels with a non-circular cross-section.

Nomenclature

A – cross-section surface, [m^2]
a – channel half width, heat diffusion coefficient ($a = \lambda/\rho c_p$),
b – buoyancy force coefficient,
c_p – specific heat, [Jkg^{-1}K^{-1}]
D – solid particles diameter, [m]
D_h – equivalent hydraulic diameter, [m]
g – gravity acceleration, [ms^{-2}]
k – kinetic turbulence energy, [m^{2}s^{-2}]
m – particle mass, [kg]
$\dot{m}$ – mass-flow, [kgs^{-1}]
P – averaged pressure, [Nm^{-2}]
∇P – continuous phase pressure gradient
$\tilde{P}$ – current pressure, [Nm^{-2}]
Re – Reynolds number,
S – source term,
T – averaged temperature, [K]
t – time step, [s]
U – averaged velocity, [ms^{-1}]
$\tilde{\mathrm{U}}$ – current velocity vector, [ms^{-1}]
$\overline{u_i u_j}$ – components of turbulent stresses,
V – averaged velocity, [ms^{-1}]
V_p – particle volume, [m^3]
W – averaged velocity, [ms^{-1}]

Greek symbols

Γ – transport, diffusion parameter coefficient
ε – dissipations of turbulent kinetic energy, [m^{2}s^{-3}]
$\overline{\eta}$ – flow of number of particles per one cell, [s^{-1}]
$\overline{\theta u_j}$ – turbulent temperature flux, [kgKm^{-2}s^{-1}]
λ – heat transfer coefficient, [Wm^{-1}K^{-1}]
ν – kinematic viscosity, [m^{2}s^{-1}]
ρ – density, [kgm^{-3}]
Φ – gas phase universal parameter

Subscripts

i, j, k – unit vectors
n – end of time step
p – particle
x, y, z – co-ordinates of position vector

Superscripts

IF – interphase term of gas and solid phase interaction
0 – beginning of time step

References

[1] Cundall, P. A., Strack, O. D. L., A Discrete Numerical Model for Granular Assemblies, *Geotechnique*, *29* (1979), 1, pp. 47-65
[2] Tsuji, Y., *et al*., Discrete Particle Simulation of Two-Dimensional Fluidized Bed, *Powder Technology*, *77* (1993), 1, pp. 79-87
[3] Zhao, X. L., *et al*., DEM Simulation of the Particle Dynamics in Two-Dimensional Spouted Beds, *Powder Technology*, *184* (2008), 2, pp. 205-213
[4] Feng, Y. Q., *et al*., Discrete Particle Simulation of Gas Fluidization of Particle Mixtures, *AIChE Journal*, *50* (2004), 8, pp. 1713-1728
[5] Campbell, C. S., Brennen, C. E., Computer Simulations of Granular Shear Flows, *Journal of Fluid Mechanics*, *151*, (1985), Feb., pp. 167-188
[6] Hoomans, B. P. B., *et al*., Discrete Particle Simulation on Bubble and Slug Formation in a Two--Dimensional Gas-Fluidised Bed: a Hard-Sphere Approach, *Chemical Engineering Science*, *51* (1996), 1, pp. 99-118
[7] Goldschmidt, M. J. V., *et al*., Hydrodynamic Modeling of Dense Gas-Fluidised Beds Using the Kinetic Theory of Granular Flow: Effect of Coefficient of Restitution on Bed Dynamics, *Chemical Engineering Science*, *56* (2001), 2, pp. 571-578
[8] Li, J., Kuipers, J. A. M., Gas-Particle Interactions in Dense Gas-Fluidized Beds, *Chemical Engineering Science*, *58* (2003), 3-6, pp. 711-718
[9] He, Y., *et al*., Gas-Solid Two-Phase Turbulent Flow in Acirculating Fluidized Bed Riser: an Experimental and Numerical Study, *Proceedings*, 5th Word Congress on Technology, Orlando, Fla., USA, 2006, pp. 1-9

[10] Tanaka, T., *et al*., Cluster Formation and Particle-Induced Instability in Gas-Solid Flows Predicted by the DSMC Method, *International Journal of JSME, 39* (1996), 2, pp. 239-245
[11] Fuzhen, C., *et al*., Coupled SDPH-FVM Method for Gas-Particle Multiphase Flow: Methodology, *International Journal for Numerical Methods in Engineering*, *109* (2017), 1, pp. 73-101
[12] Jaffari, M., *et al*., Modelling and Numerical Investigation of Erosion Rate for Turbulent Two-Phase Gas Solid Flow in Horizontal Pipes, *Powder Technology*, *267* (2014), Nov., pp. 362-370
[13] Lain, S., Study of Turbulent Two-Phase Gas-Solid Flow in Horizontal Channels, *Indian Journal of Chemical Technology*, *20* (2013), 2, pp. 128-136
[14] Schellander, D., *et al.*, Numerical Study of Dilute and Dense Poly-Dispersed Gas-Solid Two-Phase Flows Using an Eulerian-Lagrangian Hybrid Model, *Chemical Engineering Science*, *95* (2013), May, pp. 107-118
[15] Milanović, S., *et al*., The Influence of Secondary Flow in a Two-Phase Gas-Solid System in Straight Channels with a Non-Circular Cross-Section, *Thermal Science, 20* (2016), Suppl. 5, pp. S1419-S1434
[16] Hinze, J. O., *Turbulence*, McGraw-Hil, New York, USA, 1959
[17] Bird, B. R, *et al*., *Transport Phenomena*, John Wiley and Sons, New York, USA, 2001
[18] Stevanović, Ž., *Numerical Aspects of Turbulent Impulse and Heat Transfer* (in Serbian), Faculty of Mechanical Engineering, University of Nis, Nis, Serbia, 2008
[19] ***, Mathematical Models of Turbulent Transport Processes, (in Serbian), Collection of Papers Dedicated to the Academician Muhamed Rićanović, Academy of Sciences and Arts of Bosnia and Herzegovina, Sarajevo, B&H, 1984
[20] Hanjalić, K., *General Equations of Transport Processes* (in Serbian), Faculty of Mechanical Engineering, University of Sarajevo, Sarajevo, B&H, 1976
[21] Sijerčić, M., *Mathematical Modelling of Complex Turbulent Transport Processes* (in Serbian), Yugoslav Society of Thermal Engineers – Edition: Scientific Research Achievements, Belgrade, 1998
[22] Milanović, S., Research into the Turbulent Two-Phase Flow in Straight Channels with a Non-Circular Cross-Section during the Pneumatic Transport of Granular Materials, Ph. D. thesis, Faculty of Mechanical Engineering, University of Nis, Nis, Serbia, 2014
[23] Bogdanović, B., *et al*., *Flying Pneumatic Transport* (in Serbian), Faculty of Mechanical Engineering, University of Nis, Nis, Serbia, 2009
[24] Po, J. K., Developing Turbulent Flow in the Entrance Region of a Square Duct, M. Sc. thesis, University of Washington, 1975
[25] Perkins, H. J., The Formation of Streamwise Vorticity in Turbulent Flow, *Journal of Fluid Mechanics*, *44* (1970), 4, pp. 721-740

Paper submitted: April 8, 2018
Paper revised: July 24, 2018
Paper accepted: August 8, 2018